Feed-forward Space Vector Modulation for Single-Phase Multilevel Cascade Converters with any DC voltage ratio

J. I. Leon, *Member, IEEE*, S. Vazquez, *Student Member, IEEE*, A. Watson, *Student Member, IEEE*, L. G. Franquelo, *Fellow, IEEE*, P. W. Wheeler, *Member, IEEE*, J. M. Carrasco, *Member, IEEE*

***Abstract*— Modulation techniques for multilevel converters can create distorted output voltages and currents if the DC link voltages are unbalanced. This situation can be avoided if the instantaneous DC voltage error is not taken into account in the modulation process. This paper proposes a feed-forward space vector modulation method for a single-phase multilevel cascade converter. Using this modulation technique, the modulated output voltage of the power converter always generates the reference determined by the controller even in worst case voltage unbalance conditions. In addition the possibility of optimizing the DC voltage ratio between the H-bridges of the power converter is introduced. Experimental results from a 5kVA prototype are presented in order to validate the proposed modulation technique.**

***Index Terms*—Multilevel systems, Modulation, Voltage Control**

I. Introduction

MULTILEVEL cascade converters, also called cascaded H-bridge converters (CHB), have been a focus of research since they were first presented in 1988 [1]. This interest is due to their advantages compared to other multilevel converter topologies in terms of modularity and simplicity. These topologies are often used in medium and high power applications, CHB have been successfully applied in applications where a high number of levels are required with a minimum number of power semiconductors [2]-[4].

A multilevel CHB converter is composed by a series connection of H-bridges cells. For instance, a single-phase two-cell CHB converter is shown in Fig. 1. The DC link voltage ratio of a CHB converter is defined as the ratio between the DC link voltages of the cells of the converter. For example, a converter with DC voltage ratio *k:1* in a two-cell CHB means that $V_{C1}=kV_{C2}$. Depending on the number of cells in the power converter and the DC voltage ratio between the cells, the number of possible output voltage levels changes. In previous works, DC voltage ratios 1:1, 2:1 and 3:1 have been considered and the number of levels achieved by these power converter topologies has been determined [5]. One possible drawback of CHB converters with DC voltage ratio different to 1:1 is that the design of the cells may have to be different for each cell because the power ratings will be unequal between the cells. In this case, each cell has to be designed taking the voltage level into account and the converter loses its modularity.

This paper is focused on the space vector modulation (SVM) techniques for single-phase multilevel CHB converters. Previous modulation strategies do not take into account errors in the DC voltage link ratios in the modulation process and this omission leads to distorted output voltage and current waveforms. Using previous techniques, the modulator does not actually follow the reference determined by the controller leading to waveform distortion. This waveform distortion is avoided using the proposed feed-forward modulation technique.

II. Modulation techniques for CHB converters

Different multilevel modulation techniques for CHB converters have been presented in the literature. Many of these techniques have been extended from classic pulse width modulation (PWM) and space vector modulation (SVM) methods. Level-shifted PWM and phase-shifted PWM are derived from classic PWM methods that use triangular carriers [6]-[8]. In [9] it is reported that the phase-shifted PWM modulation is the natural method for CHB converters achieving good quality output voltage with a fundamental component N times the fundamental component of each cell for an N-cell CHB converter. Multilevel SVM techniques have been presented and achieve simplicity offering an alternative to carrier based PWM techniques [10]-[14].

Manuscript received October 31, 2007. Accepted for publication April 22, 2008. This work was supported in part by the Spanish Ministry of Education and Science under Project TEC2006-03863.

J. I. Leon, S. Vazquez, L. G. Franquelo and J. M. Carrasco are with the Electronic Engineering Department of the University of Seville, 41092, Seville (Spain) (phone: 0034-954481312; fax: 0034-954487373; e-mail: jileon@gte.esi.us.es).

A. Watson and P. Wheeler are with the School of Electrical and Electronic Engineering, The University of Nottingham, NG7 2RD Nottingham, U.K. (e-mail:pat.wheeler@nottingham.ac.uk; http://www.eee.nottingham.ac.uk).

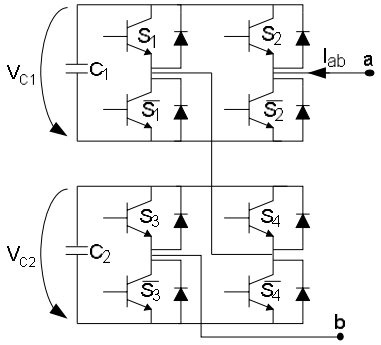

Fig. 1. Two-cell single-phase CHB converter with any DC voltage

SVM strategies are based on the generation of the reference voltage determined by the controller as an average of the discrete output voltages that can be achieved by the power converter. These techniques take advantage of the degrees of freedom as the selection of the switching sequence can be made in order to improve some power converter feature as the number of commutations or voltage balance [15][16].

However, both the PWM and SVM methods have problems when the multilevel converter is operated with uncontrolled DC-Link voltages. With CHB converters, if the DC voltages are not of the correct magnitude and the modulators do not take these voltage errors into account there will be distortion in the output waveforms. This problem can be avoided in single-phase multilevel CHB converters using the feed-forward SVM technique presented in this paper.

III. 1D CONTROL REGION FOR MULTILEVEL CHB CONVERTERS

The control region of a single-phase converter can be represented as a 1D control region [17]. In [17] a single-phase diode-clamped multilevel converter is studied where the control region is represented as a line showing where the possible states of the converter are located. The definition of this 1D control region is the base of the proposed SVM technique for single-phase multilevel CHB converters.

In order to introduce the calculation of the control region for single-phase multilevel CHB converters the two-cell case represented in Fig. 1 is studied. The output phase voltage depends on the output voltage of each cell of the converter, therefore the output phase voltage $V_{ab}=V_{m1}+V_{m2}$ where V_{m1} and V_{m2} are the output voltages of upper and lower cell respectively.

The output of each H-bridge can take any of three different output voltages, $-V_{Ci}$, 0 and V_{Ci}, defined as H-bridge states 0, 1 and 2 respectively. As the output phase voltage is composed of the sum of the cell output voltages, in the two-cell single-phase CHB converter five output voltages can be achieved. Assuming that $V_{C1}=V_{C2}=E$, these output voltage levels are shown in Table I. Some redundant states appear in the CHB power converter because the same output voltage can be achieved using different combinations of individual H-bridge states.

Using Table I it is possible to represent the control region of the single-phase two-cell CHB converter. Output phase voltage V_{ab} is used as the component to be plotted. In addition, the cell states can be placed in the 1D representation taking into account their corresponding contribution to the output phase voltage. Finally, the control region of the two-cell CHB converter is represented in Fig. 2. State vector *XY* means that the upper cell has state *X* and the lower cell has state *Y*. The presence of redundant state vectors is clear using this representation because different H-bridge states are located in the same point of the control region. For instance, to achieve $V_{ab}=E$, two different state vectors (12 and 21) can be used.

IV. 1D-SVM TECHNIQUE FOR MULTILEVEL SINGLE-PHASE CHB CONVERTERS ASSUMING EQUAL DC VOLTAGES

Using the 1D control region introduced in Fig. 2 for two-cell single-phase CHB converters with equal DC voltages, a 1D-SVM strategy can be developed using the nearest two vectors (N2V) method. The N2V technique achieves the generation of the reference voltage (V_{ab_ref}) using the two nearest state vectors in the control region. For instance, if V_{ab_ref} is equal to 1.7E, the 1D-SVM strategy uses state vectors {22-12} or {22-21} as the switching sequence because if V_{ab_ref} is represented in the 1D control region, it is located between these state vectors. The reference vector is generated using a linear combination of the two nearest state vectors of the control region. The flow diagram of the proposed 1D-SVM technique to carry out the determination of the switching sequence and the corresponding duty cycles is shown in Fig. 3. Operator *floor(x)* rounds the elements of *x* to the nearest integers towards minus infinity. The switching sequence is formed by states upper_1-lower_1 and upper_2-lower_2 with duty cycles t_1 and t_2 respectively. The redundancy of the H-bridge states is not taken into account and one possible state vector is chosen.

TABLE I
OUTPUT PHASE VOLTAGES OF THE TWO-CELL SINGLE-PHASE CHB CONVERTER ASSUMING E VOLTS IN EACH H-BRIDGE

Upper H-bridge state	Lower H-bridge state	Output Phase Voltage (V_{ab})
0	0	-2E
0	1	-E
1	0	-E
0	2	0
1	1	0
2	0	0
1	2	E
2	1	E
2	2	2E

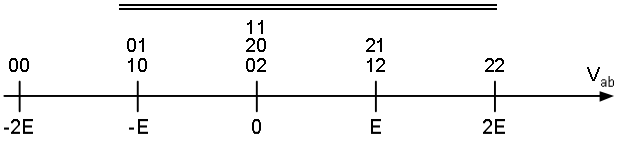

Fig. 2. Control region of a two-cell single-phase CHB converter assuming voltage E in each H-bridge

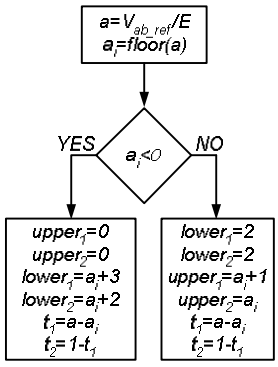

Fig. 3. Flow diagram of the 1D-SVM for the two-cell single-phase CHB converter assuming voltage E in each H-bridge

V. Experimental Results of the Proposed 1D-SVM

In order to validate the proposed modulation technique some experimental results have been obtained using the prototype depicted in Fig. 4. In the experiment, the CHB converter is connected to a 130V (peak) supply and is working as an inverter delivering approximately 1A of current to a RL load (R=126Ω and L=35.5mH) using 10 kHz of switching frequency. The DC voltage ratio is 1:1 with V_{DC1}=V_{DC2}=75V. The output modulated voltage and the current through the inductor are shown in Fig. 5a and Fig. 5b respectively. The harmonic spectrum of the output voltage up to 15 kHz is represented in Fig. 5c. The total harmonic distortion (THD) of the output voltage considering up to 15 kHz harmonic is 30.68%

The proposed 1D-SVM can be used for two-cell CHB converters in a balanced situation, i.e. when the DC voltages of each cell (V_{C1},V_{C2}) are equal. If the DC voltages of the power converter are not equal, the reference waveform will not be correct because the assumptions in Table I would not be true and the 1D control region would change. If the flow diagram shown in Fig. 3 is used for unbalanced DC voltage conditions, the averaged output voltage will not be the desired reference voltage and undesirable distortion appears in the output voltage. This phenomenon is shown in Fig. 6 where the experiment of Fig. 5 is repeated but forcing a DC voltage unbalance in the prototype imposing V_{C1}=50V and V_{C2}=100V. As this voltage unbalance is not taken into account in the modulation process, the output modulated voltage presents a clear distortion resulting in distortion of the current waveform shown in Fig. 6b. This distortion has been measured showing the harmonic spectrum of the output voltage up to 15 KHz in Fig. 6c. The total harmonic distortion (THD) of the output voltage considering up to 15 kHz harmonic is 43.57% and the distortion of third order harmonic is 10%.

A new SVM technique taking into account the instantaneous DC voltages of the power converter has been developed in order to avoid the distortion in the output waveforms under unbalanced DC voltage conditions.

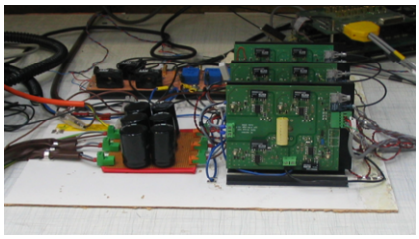

Fig. 4. Two cell CHB converter prototype used in experimental verification of modulation strategy (Third cell disconnected).

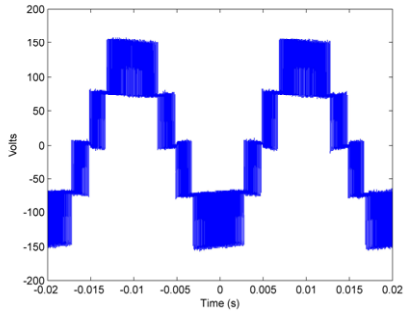

(a)

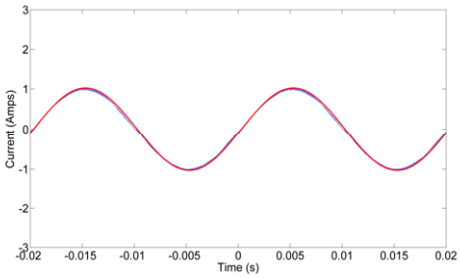

(b)

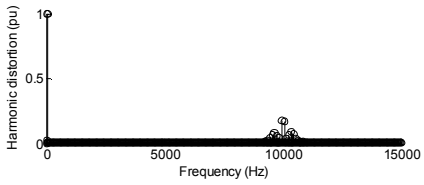

(c)

Fig. 5. Experimental results for the 1D-SVM technique using a two-cell CHB converter with V_{C1}=V_{C2}=75 V. (a) Output modulated voltage (b) 1A current delivered to the RL load (c) Harmonic spectrum of the output voltage

VI. 1D Control Region of Multilevel CHB Converters with any DC Voltage

The two-cell single-phase CHB converter can be considered assuming that any cell can take any DC voltage. In general, each H-bridge has a DC voltage defined by V_{Ci} and the nine possible output voltages of the converter are summarized in Table II. In this generalized case, the control region can again be represented using one dimension but mapping the states created by the variation in the DC voltages of the cells. Previous authors have presented feed-forward SVM techniques for three-level diode-clamped converters when the DC-Link voltage become unbalanced [18][19]. This feed-forward modulation technique is based on the calculation of the control region of the power converter taking into account the instantaneous voltage of each DC-Link capacitor.

TABLE II
OUTPUT PHASE VOLTAGES OF THE TWO-CELL SINGLE-PHASE CHB CONVERTER WITH ANY DC VOLTAGE IN EACH H-BRIDGE

Upper H-bridge state	Lower H-bridge state	Output Phase Voltage (V_{ab})
0	0	$-V_{C1}-V_{C2}$
0	1	$-V_{C1}$
1	0	$-V_{C2}$
0	2	$-V_{C1}+V_{C2}$
1	1	0
2	0	$V_{C1}-V_{C2}$
1	2	V_{C2}
2	1	V_{C1}
2	2	$V_{C1}+V_{C2}$

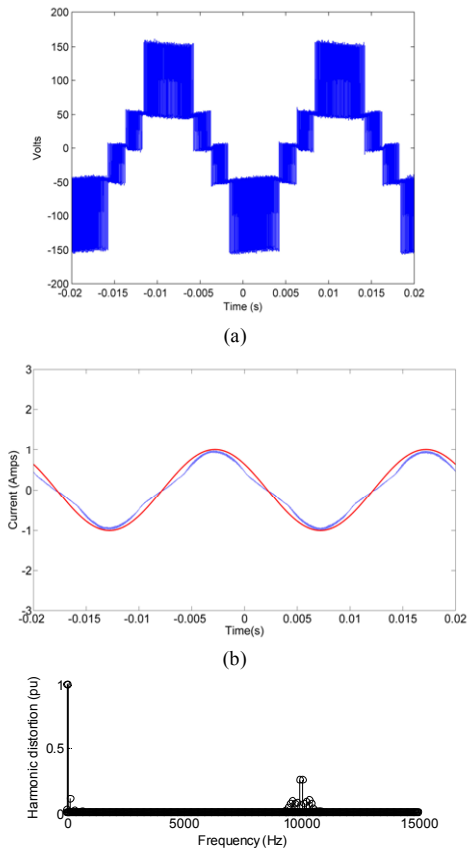

Fig. 6. Experimental results for the 1D-SVM technique using a two-cell CHB converter with V_{C1}=50 V and V_{C2}=100 V. (a) Output modulated voltage (b) 1A demanded current not met and waveform distorted due to voltage imbalance (c) Harmonic spectrum of the output voltage

The calculation of the switching sequence and the duty cycles is made using this control region determined online. A feed-forward multicarrier PWM strategy has been presented in [20]. A similar idea has been applied to multilevel single-phase CHB converters to develop the proposed 1D feed-forward SVM (1D-FFSVM) technique. In the single-phase two-cell CHB converter case using the feed-forward process the movement of the state vectors from the voltage balanced position shown in Fig. 2 can be represented to show how the 1D control region changes as voltages become unbalanced. Four different cases (see Fig. 7 to Fig. 10) appear because depending on the instantaneous voltage unbalance, the order or the state vectors from the most negative to the most positive is different. The movement of the state vectors from the voltage balanced case is represented in Fig. 7a to Fig. 10a. In addition, the feed-forward control region of the single-phase two-cell CHB converter is shown in Fig. 7b to Fig. 10b. In each case, factors k_1, k_2 and k_3 are defined as the positive output voltages of the state vectors normalized using the total DC voltage of the converter $V_{C1}+V_{C2}$. Depending on the case number, k_i factors are defined using Table III.

Case 1: $V_{C2}<V_{C1}<2V_{C2}$

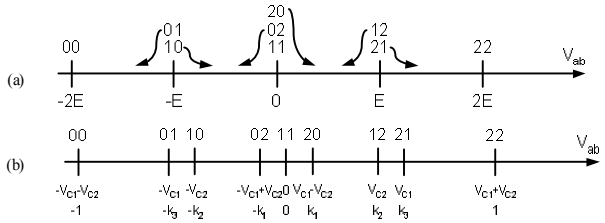

Fig. 7. (a) Movement of the state vectors due to the voltage unbalance when $V_{C2}<V_{C1}<2V_{C2}$ (b) Control region of the two-cell single-phase CHB converter with unbalanced voltages fulfilling $V_{C2}<V_{C1}<2V_{C2}$.

Case 2: $V_{C1}>2V_{C2}$

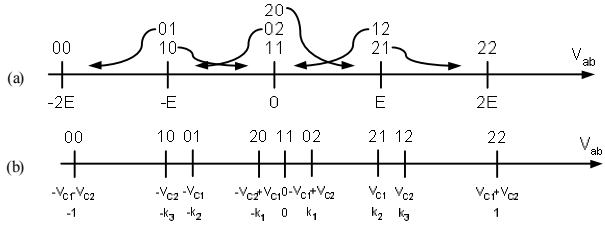

Fig. 8. (a) Movement of the state vectors due to the voltage unbalance when $V_{C1}>2V_{C2}$ (b) Control region of the two-cell single-phase CHB converter with unbalanced voltages fulfilling $V_{C1}>2V_{C2}$

Case 3: $V_{C1}<V_{C2}<2V_{C1}$

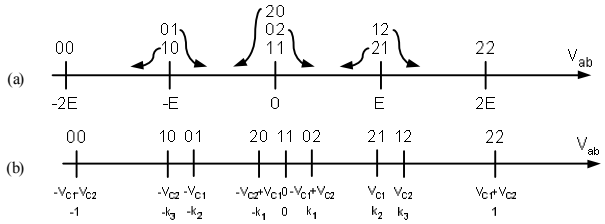

Fig. 9. (a) Movement of the state vectors due to the voltage unbalance when $V_{C1}<V_{C2}<2V_{C1}$ (b) Control region of the two-cell single-phase CHB converter with unbalanced voltages fulfilling $V_{C1}<V_{C2}<2V_{C1}$

Case 4: $V_{C2}>2V_{C1}$

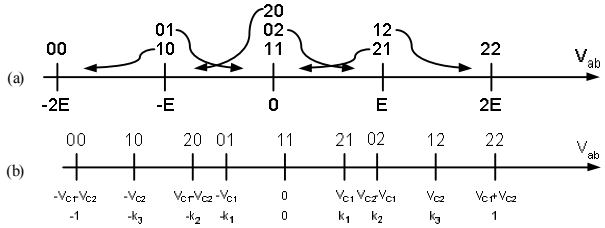

Fig. 10. (a) Movement of the state vectors due to the voltage unbalance when $V_{C2}>2V_{C1}$ (b) Control region of the two-cell single-phase CHB converter with unbalanced voltages fulfilling $V_{C2}>2V_{C1}$

VII. Feed-forward SVM technique for two-cell CHB converters with any DC voltage

A generalized feed-forward 1D-SVM (1D-FFSVM) can be developed including all the cases with any unbalance in the DC voltages. Using this 1D-FFSVM technique, any voltage unbalance does not affect the output voltage of the converter because the instantaneous unbalance is taken into account in the modulation process. In this way, the undesirable distortion in the output voltage and current waveforms is avoided.

The first step of the proposed 1D-FFSVM method is the normalization of the output phase reference voltage (V_{ab_ref}) determined by an external controller using the following expression:

$$a = \frac{V_{ab\_ref}}{V_{C1} + V_{C2}} \tag{1}$$

The second step of the algorithm is to measure the instantaneous DC voltages of the power converter and to determine the case (cases 1-4) where the converter is working. Once the case is known, k_i factors can be determined using the equations presented in Table III.

The third and final step of the algorithm uses these k_i factors to determine the position of the reference vector in the 1D control region calculating the switching sequence and the corresponding duty cycles. These calculations are summarized in Table IV and Table V for negative and positive values of a respectively. The switching sequence is formed by a sequence where each H-bridge changes its state one time per switching period. The switching sequence is denoted as $upper_1lower_1$-$upper_2lower_2$. Duty cycle t_1 is the time for state $upper_1lower_1$ and t_2 is always equal to 1-t_1 and it is the time for state $upper_2lower_2$.

The proposed 1D-FFSVM for two-cell single-phase CHB can be easily extended when the number of cells is increased. Using similar calculations, the feed-forward SVM algorithm can be developed. In the M-cell case, 3^M state vectors are placed in the control region. The modulation strategy finds out the nearest state vectors with an iterative search to determine the switching sequence. The corresponding duty cycles are then calculated defining the necessary k_i, i=1,2,…,(3^M-3)/2, and defining the tables for the possible 3^M-1 cases of the position of factor a in the control region. Therefore, it must be noticed that the number of cases to consider in the modulation strategy increases with the number of cells in the power converter. The computational cost of the 1D-FFSVM method is only slightly increased because all cases can be considered using the necessary tables. Therefore, only the iterative search of the 1D-FFSVM strategy depends on the number of cells of the power converter.

VIII. Experimental results of the proposed 1D-FFSVM

The prototype of the two-cell single-phase CHB converter shown in Fig. 4 has been used to test the proposed 1D-FFSVM technique.

TABLE III
K_1, K_2 AND K_3 FACTORS CALCULATION

Case number	Voltage Condition	k_i factors definition
1	$V_{C2}<V_{C1}<2V_{C2}$	$k_1= (V_{C1}-V_{C2})/(V_{C1}+V_{C2})$ $k_2= V_{C2}/(V_{C1}+V_{C2})$ $k_3= V_{C1}/(V_{C1}+V_{C2})$
2	$V_{C1}>2V_{C2}$	$k_1= V_{C2}/(V_{C1}+V_{C2})$ $k_2= (V_{C1}-V_{C2})/ (V_{C1}+V_{C2})$ $k_3= V_{C1}/(V_{C1}+V_{C2})$
3	$V_{C1}<V_{C2}<2V_{C1}$	$k_1= (V_{C2}-V_{C1})/ (V_{C1}+V_{C2})$ $k_2= V_{C1}/(V_{C1}+V_{C2})$ $k_3= V_{C2}/(V_{C1}+V_{C2})$
4	$V_{C2}>2V_{C1}$	$k_1= V_{C1}/(V_{C1}+V_{C2})$ $k_2= (V_{C2}-V_{C1})/ (V_{C1}+V_{C2})$ $k_3= V_{C2}/(V_{C1}+V_{C2})$

TABLE IV
SWITCHING SEQUENCE AND DUTY CYCLES IF THE NORMALIZED REFERENCE VECTOR IS NEGATIVE

Case	Case number	Switching sequence	Duty cycles
$0>a>-k_1$	1	11-02	$t_1=(a+k_1)/k_1$
	2	11-10	
	3	11-20	
	4	11-01	
$-k_1>a>-k_2$	1	02-10	$t_1=(a+k_2)/(k_2-k_1)$
	2	10-02	
	3	20-01	
	4	01-20	
$-k_2>a>-k_3$	1	10-01	$t_1=(a+k_3)/(k_3-k_2)$
	2	02-01	
	3	01-10	
	4	20-10	
$-k_3>a>-1$	1	01-00	$t_1=(a+1)/(1-k_3)$
	2	01-00	
	3	10-00	
	4	10-00	

TABLE V
SWITCHING SEQUENCE AND DUTY CYCLES IF THE NORMALIZED REFERENCE VECTOR IS POSITIVE

Case	Case number	Switching sequence	Duty cycles
$k_1>a>0$	1	20-11	$t_1=a/k_1$
	2	12-11	
	3	02-11	
	4	21-11	
$k_2>a>k_1$	1	12-20	$t_1=(a-k_1)/(k_2-k_1)$
	2	20-12	
	3	21-02	
	4	02-21	
$k_3>a>k_2$	1	21-12	$t_1=(a-k_2)/(k_3-k_2)$
	2	21-20	
	3	12-21	
	4	12-02	
$1>a>k_3$	1	22-21	$t_1=(a-k_3)/(1-k_3)$
	2	22-21	
	3	22-12	
	4	22-12	

The same experimental conditions presented in Fig. 6 have been performed using the 1D-FFSVM method in order to compare the results with the previous 1D-SVM strategy. Note that under this strategy, due to the nature of different cell states which do not switch simultaneously, certain applied states may result in output waveform distortion. For example, if we require the total converter voltage of zero and we apply a state where the first cell applies E and the second –E, if these

states do not change at exactly the same time (i.e. due a small difference in commutation time) a narrow pulse of E or –E will occur in the total waveform, thus distorting it. These narrow pulses have been removed from the inverter results to show clarity by applying a filter to the scope used to take the measurements. It is clear however that they do not significantly distort the current.

The unbalanced experimental results are shown in Fig. 11, where different DC voltages are applied to the CHB converter (V_{DC1}=50V and V_{DC2}=100V). Compared with the previous method (see Fig. 6), under an unbalanced situation, the new feed-forward strategy achieves demanded current whilst avoiding the distortion in the output voltage waveform and therefore reducing the errors in the current tracking. Using the proposed 1D-FFSVM method, the total harmonic distortion (THD) of the output voltage considering up to 15 kHz harmonic is 18.16%.

IX. 1D-FFSVM Technique for Multilevel CHB Converters with DC Voltage Ratio Control. DC Voltage Ratio 1:1

Other previously published works have demonstrated that the SVM techniques can provide the balance of the voltages for different multilevel converter topologies [21]-[23]. A similar method to achieve the desired DC voltages in the two-cell single-phase converter using the proposed 1D-FFSVM strategy is presented in this paper.

In this study, the control objective is to have the same voltage in each cell of the power converter. The effect of each state on the capacitors DC voltage can be predicted and all the possibilities are shown in Table VI where depending on the H-bridge state and the sign of the phase current I_{ab}, the capacitor voltage will increase or decrease. This calculation is well known and is applied to multilevel converters along with the concept of the redundant vectors in the SVM strategies to control the DC voltages of the DC-Link in different multilevel converter topologies [24]-[26].

In the CHB case with any DC voltage value, the proposed way to control the balance of the DC voltages is to forbid the use of the inappropriate states in the switching sequence regardless of whether or not they are redundant. In this way, only the H-bridge states which do not unbalance the DC voltages are allowed to be used. Therefore, a new 1D-FFSVM technique is developed eliminating the inappropriate states and making the system tends to the equilibrium. Different cases have to be studied depending on the instantaneous DC voltage unbalance and the sign of the phase current. For instance, if I_{ab}>0 and V_{C2}<V_{C1}<2V_{C2}, state vectors 10, 20 and 21 are forbidden because they tend to decrease V_{C2} or increase V_{C1} leading to increase the DC voltage unbalance in the power converter. This specific example is shown in Fig. 12. All the cases can be studied in the same way and the resulting control regions are shown in Fig. 12 to Fig. 19. As the 1D control region changes, the third step of the 1D-FFSVM has to change in order to use only the proper states of the control region. The determination of the switching sequence and the duty cycles is summarized for each case using tables from Table VII to Table XIV.

TABLE VI
Influence of the Switching in the H-Bridge on the H-Bridge Capacitor Voltage

H-bridge state	Output H-bridge Voltage	Influence on V_{Ci} with I_{ab}>0	Influence on V_{Ci} with I_{ab}<0
0	$-V_{Ci}$	↓	↑
1	0	—	—
2	V_{Ci}	↑	↓

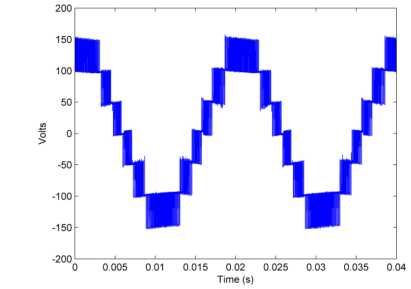

(a)

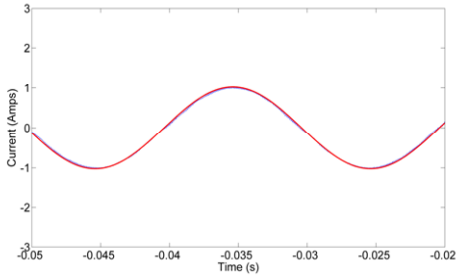

(b)

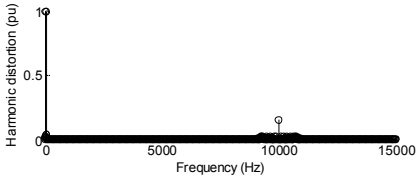

(c)

Fig. 11. Experimental results for the 1D-FFSVM technique using a two-cell CHB converter with V_{C1}=50 V and V_{C2}=100 V. (a) Output modulated voltage (b) 1A current delivered to the RL load (c) Harmonic spectrum of the output voltage

A. I_{ab}>0, V_{C2}<V_{C1}<2V_{C2}

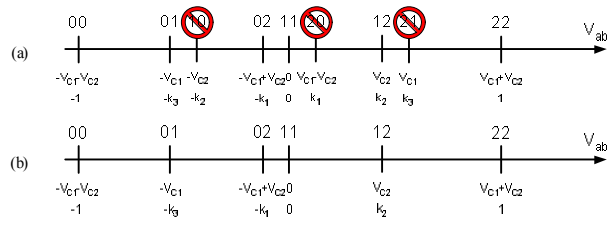

Fig. 12. (a) Movement of the state vectors due to the voltage unbalance when V_{C2}<V_{C1}<2V_{C2} (b) 1D control region searching the DC voltage ratio 1:1 (V_{C1}=V_{C2}) of the two-cell single-phase CHB converter with unbalanced DC voltages fulfilling V_{C2}<V_{C1}<2V_{C2} and I_{ab}>0. State vectors 10, 20 and 21 are not used.

TABLE VII
SWITCHING SEQUENCE AND DUTY CYCLES WITH $V_{C2}<V_{C1}<2V_{C2}$ AND $I_{AB}>0$

Case	Duty cycles	Switching sequence
$-k_3>a>-1$	$t_1=(a+1)/(1-k_3)$	01-00
$-k_1>a>-k_3$	$t1=(a+k_3)/(k_3-k_1)$	02-01
$0>a>-k_1$	$t1=(a+k_1)/k_1$	11-02
$k_2>a>0$	$t1=a/k_2$	12-11
$1>a>k_2$	$t1=(a-k_2)/(1-k_2)$	22-12

B. $I_{ab}>0$, $V_{C1}>2V_{C2}$

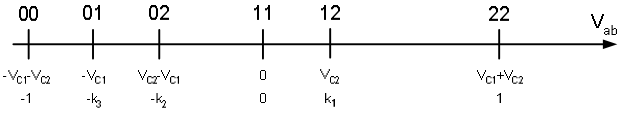

Fig. 13. 1D control region searching the DC voltage ratio 1:1 ($V_{C1}=V_{C2}$) of the two-cell single-phase CHB converter with unbalanced DC voltages fulfilling $V_{C1}>2V_{C2}$ and $I_{ab}>0$. State vectors 10, 20 and 21 are not used.

TABLE VIII
SWITCHING SEQUENCE AND DUTY CYCLES WITH $V_{C1}>2V_{C2}$ AND $I_{AB}>0$

Case	Duty cycles	Switching sequence
$-k_3>a>-1$	$t_1=(a+1)/(1-k_3)$	01-00
$-k_2>a>-k_3$	$t_1=(a+k_3)/(k_3-k_2)$	02-01
$0>a>-k_2$	$t_1=(a+k_2)/k_2$	11-02
$k_1>a>0$	$t_1=a/k_1$	12-11
$1>a>k_1$	$t_1=(a-k_1)/(1-k_1)$	22-12

C. $I_{ab}>0$, $V_{C1}<V_{C2}<2V_{C1}$

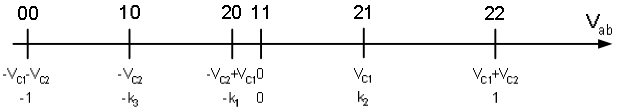

Fig. 14. 1D control region searching the DC voltage ratio 1:1 ($V_{C1}=V_{C2}$) of the two-cell single-phase CHB converter with unbalanced DC voltages fulfilling $V_{C1}<V_{C2}<2V_{C1}$ and Iab>0. State vectors 01, 02 and 12 are not used.

TABLE IX
SWITCHING SEQUENCE AND DUTY CYCLES WITH $V_{C1}<V_{C2}<2V_{C1}$ AND $I_{AB}>0$

Case	Duty cycles	Switching sequence
$-k_3>a>-1$	$t_1=(a+1)/(1-k_3)$	10-00
$-k_1>a>-k_3$	$t_1=(a+k_3)/(k_3-k_1)$	20-10
$0>a>-k_1$	$t_1=(a+k_1)/k_1$	11-20
$k_2>a>0$	$t_1=a/k_2$	21-11
$1>a>k_2$	$t_1=(a-k_2)/(1-k_2)$	22-21

D. $I_{ab}>0$, $V_{C2}>2V_{C1}$

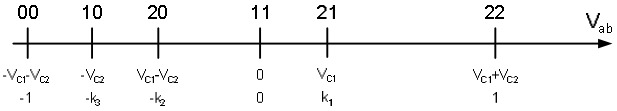

Fig. 15. 1D control region searching the DC voltage ratio 1:1 ($V_{C1}=V_{C2}$) of the two-cell single-phase CHB converter with unbalanced DC voltages fulfilling $V_{C2}>2V_{C1}$ and Iab>0. State vectors 01, 02 and 12 are not used.

TABLE X
SWITCHING SEQUENCE AND DUTY CYCLES WITH $V_{C2}<2V_{C1}$ AND $I_{AB}>0$

Case	Duty cycles	Switching sequence
$-k_3>a>-1$	$t_1=(a+1)/(1-k_3)$	10-00
$-k_2>a>-k_3$	$t_1=(a+k_3)/(k_3-k_2)$	20-10
$0>a>-k_2$	$t_1=(a+k_2)/k_2$	11-20
$k_1>a>0$	$t_1=a/k_1$	21-11
$1>a>k_1$	$t_1=(a-k_1)/(1-k_1)$	22-21

E. $I_{ab}<0$, $V_{C2}<VC1<2V_{C2}$

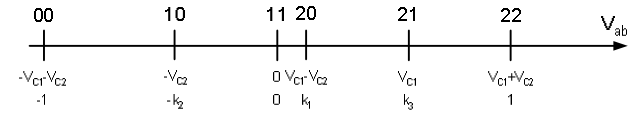

Fig. 16. 1D control region searching the DC voltage ratio 1:1 ($V_{C1}=V_{C2}$) of the two-cell single-phase CHB converter with unbalanced DC voltages fulfilling $V_{C2}<V_{C1}<2V_{C2}$ and $I_{ab}<0$. State vectors 01, 02 and 12 are not used.

TABLE XI
SWITCHING SEQUENCE AND DUTY CYCLES WITH $V_{C2}<V_{C1}<2V_{C2}$ AND $I_{AB}<0$

Case	Duty cycles	Switching sequence
$-k_2>a>-1$	$t_1=(a+1)/(1-k_2)$	10-00
$0>a>-k_2$	$t_1=(a+k_2)/k_2$	11-10
$k_1>a>0$	$t_1=a/k_1$	20-11
$k_3>a>k_1$	$t_1=(a-k_1)/(k_3-k_1)$	21-20
$1>a>k_3$	$t_1=(a-k_3)/(1-k_3)$	22-21

F. $I_{ab}<0$, $V_{C1}>2V_{C2}$

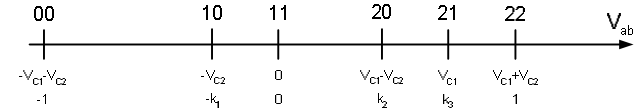

Fig. 17. 1D control region searching the DC voltage ratio 1:1 ($V_{C1}=V_{C2}$) of the two-cell single-phase CHB converter with unbalanced DC voltages fulfilling $V_{C1}>2V_{C2}$ and $I_{ab}<0$. State vectors 01, 02 and 12 are not used.

TABLE XII
SWITCHING SEQUENCE AND DUTY CYCLES WITH $V_{C1}>2V_{C2}$ AND $I_{AB}<0$

Case	Duty cycles	Switching sequence
$-k_1>a>-1$	$t_1=(a+1)/(1-k_1)$	10-00
$0>a>-k_1$	$t_1=(a+k_1)/k_1$	11-10
$k_2>a>0$	$t_1=a/k_2$	20-11
$k_3>a>k_2$	$t_1=(a-k_2)/(k_3-k_2)$	21-20
$1>a>k_3$	$t_1=(a-k_3)/(1-k_3)$	22-21

G. $I_{ab}<0$, $V_{C1}<V_{C2}<2V_{C1}$

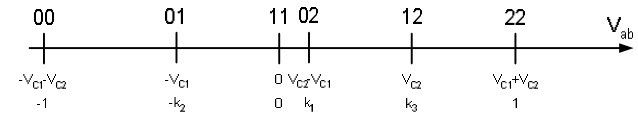

Fig. 18. 1D control region searching the DC voltage ratio 1:1 ($V_{C1}=V_{C2}$) of the two-cell single-phase CHB converter with unbalanced DC voltages fulfilling $V_{C1}<V_{C2}<2V_{C1}$ and $I_{ab}<0$. State vectors 10, 20 and 21 are not used.

TABLE XIII
SWITCHING SEQUENCE AND DUTY CYCLES WITH $V_{C1}<V_{C2}<2V_{C1}$ AND $I_{AB}<0$

Case	Duty cycles	Switching sequence
$-k_2>a>-1$	$t_1=(a+1)/(1-k_2)$	01-00
$0>a>-k_2$	$t_1=(a+k_2)/k_2$	11-01
$k_1>a>0$	$t_1=a/k_1$	02-11
$k_3>a>k_1$	$t_1=(a-k_1)/(k_3-k_1)$	12-02
$1>a>k_3$	$t_1=(a-k_3)/(1-k_3)$	22-12

H. $I_{ab}<0$, $V_{C2}>2V_{C1}$

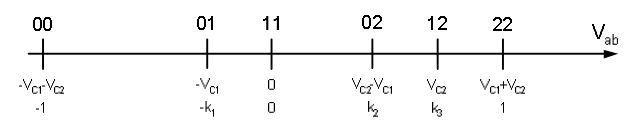

Fig. 19. 1D control region searching the DC voltage ratio 1:1 ($V_{C1}=V_{C2}$) of the two-cell single-phase CHB converter with unbalanced DC voltages fulfilling $V_{C2}>2V_{C1}$ and $I_{ab}<0$. State vectors 10, 20 and 21 are not used.

TABLE XIV
SWITCHING SEQUENCE AND DUTY CYCLES WITH $V_{C2}>2V_{C1}$ AND $I_{AB}<0$

Case	Duty cycles	Switching sequence
$-k_1>a>-1$	$t_1=(a+1)/(1-k_1)$	01-00
$0>a>-k_1$	$t_1=(a+k_1)/k_1$	11-01
$k_2>a>0$	$t_1=a/k_2$	02-11
$k_3>a>k_2$	$t_1=(a-k_2)/(k_3-k_2)$	12-02
$1>a>k_3$	$t_1=(a-k_3)/(1-k_3)$	22-12

The proposed strategy to balance the DC voltages using the 1D-FFSVM has been tested. The experimental results are shown in Fig. 20. Fig. 20a shows a result of disabling the proposed technique and re-enabling it a few seconds later. It is clear that without the technique unequal power flow into the converter cells will result in voltage divergence. However when the 1D-FFSVM technique is applied, the DC link capacitor voltages are converged ($V_{C1}=V_{C2}=75V$). In Fig. 20b, the modulated output voltage, the supply voltage and the output current are shown. It is clear that the current is of a high quality and that the DC link capacitor voltages have been converged by the technique since the converter voltage increases in equal voltage steps. This distortion, which is due to delays in switching from one state to another, is shown in the first half cycle of the converter waveform shown in Fig. 20b. It is clear that this does not have a significant effect on the current. The harmonic spectrum of the output voltage up to 15 KHz is shown in Fig. 20c. The total harmonic distortion (THD) of the output voltage considering up to 15 kHz harmonic is 27.09%. It can be seen that good results are obtained with the proposed 1D-FFSVM strategy applied to the two-cell CHB converter working as a controlled rectifier with a desired DC voltage ratio equal to 1:1.

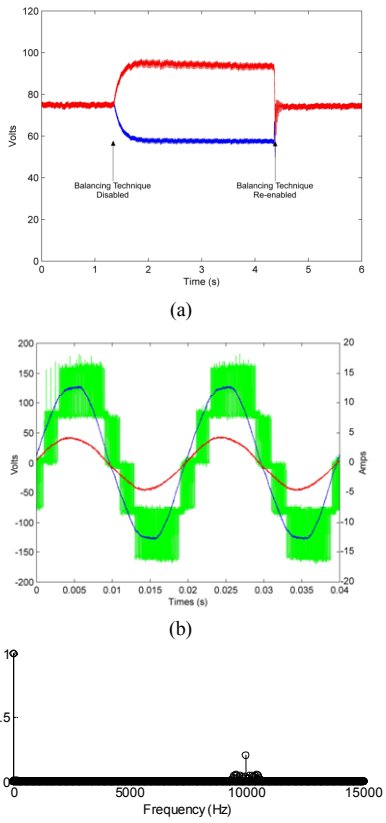

Fig. 20. Experimental results for the optimized 1D-FFSVM technique using a two-cell single-phase CHB converter. DC voltage ratio control objective is 1:1 ($V_{C1}=V_{C2}=75$ V). (a) DC voltages when the balancing scheme is disabled and re-enabled. (b) Output modulated voltage (G), Supply voltage (B) and output current (R) (c) Harmonic spectrum of the output voltage per unit

X. 1D-FFSVM TECHNIQUE FOR MULTILEVEL CHB CONVERTERS WITH ANY DC VOLTAGE RATIO CONTROL.

All possible DC voltage ratios can be reduced to the 8 cases (cases from A to H) as previously studied in the balanced case. Depending on the instantaneous DC voltage unbalance and the sign of the phase current, a case has to be applied in order to ensure that the power flowing into the converter forces the overall DC voltage to tend to the desired voltage ratio. As an example, the DC voltage ratio 3:1 results are summarized in Table XV where depending on the DC voltage unbalance and the sign of the phase current the DC voltage ratio 1:1 case to be applied is shown.

The control strategy to achieve DC voltage ratio 3:1 using the 1D-FFSVM has been experimentally tested. The results are shown in Fig. 21. From Fig. 21a, it is clear that the steady state values of total rectifier has been reached and that the 3:1 ratio is achieved, since $V_{C1}=120V$ and $V_{C2}=40V$. It is also clear that from Fig. 21b that the rectifier has achieved a high quality current at unity displacement factor while the output voltage is slightly distorted.

TABLE XV
DC VOLTAGE RATIO 1:1 CASE TO BE APPLIED WITH THE OBJECTIVE DC VOLTAGE RATIO 3:1

Current/Voltage condition	Associated balanced case
$I_{ab}>0$, $V_{C2}<V_{C1}<2V_{C2}$	E
$I_{ab}>0$, $3V_{C2}>V_{C1}>2V_{C2}$	F
$I_{ab}>0$, $V_{C1}>3V_{C2}$	B
$I_{ab}>0$, $V_{C1}<V_{C2}<2V_{C1}$	C
$I_{ab}>0$, $V_{C2}>2V_{C1}$	D
$I_{ab}<0$, $V_{C2}<V_{C1}<2V_{C2}$	A
$I_{ab}<0$, $2V_{C2}<V_{C1}<3V_{C2}$	B
$I_{ab}<0$, $V_{C1}>3V_{C2}$	F
$I_{ab}<0$, $V_{C1}<V_{C2}<2V_{C1}$	G
$I_{ab}<0$, $2V_{C1}<V_{C2}<3V_{C1}$	H

The output voltage distortion depends on the chosen DC voltage ratio and does not depend on the load conditions. Using voltage ratio 3:1 the output line-to-line voltage becomes deteriorated because some states are avoided in the switching of the power converter and due to the ratio 3:1 the redundancy property is lost. Using other DC voltage ratios such as 1:1 the redundancy property permits to achieve the desired output voltage using voltage levels as can be seen in Fig. 20b.

In order to compare the results with both DC voltage ratios, in Fig. 21c the harmonic spectrum of the output voltage is

shown. The total harmonic distortion (THD) of the output voltage considering up to 15 kHz harmonic is 20.41%. It can be seen that using DC voltage ratio 3:1 the obtained harmonic spectrum improves the results of ratio 1:1. This phenomenon is due to the increase of the number of levels of the output voltage. The proposed 1D-FFSVM with the DC voltage ratio control for two-cell single-phase CHB can be also extended when the number of cells of the power converter is increased. It can be said that increasing the number of cells, the number of cases to study increases as well. However, all the calculations can be done offline determining all the necessary tables to be used in the modulation process. The computational cost of the DC voltage ratio control algorithm is not increased when more cells are added to the power system. Thus, only the iterative search of the 1DFFSVM algorithm depends on the number of cells of the converter increasing the computational cost.

XI. CONCLUSIONS

A simple and generalized feed-forward space vector modulation (1D-FFSVM) technique for multilevel single-phase cascade converters (CHB) has been presented. Using the proposed modulation strategy, any DC voltage ratio in the CHB converter can be accommodated in the modulation process to generate the reference voltage.

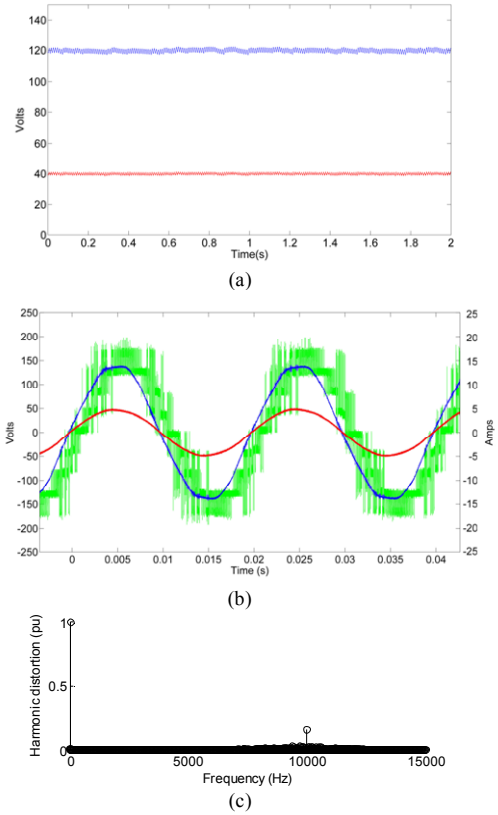

Fig. 21. Experimental results for the 1D-FFSVM technique using a two-cell CHB converter with DC voltage control. (a) DC voltages shown for ratio 3:1 (120V:40V) for a 160V DC demand. (b) Output modulated voltage (G), Supply voltage (B) and output current (R) (c) Harmonic spectrum of the output voltage per unit

The controller determines the best output voltage of the power converter and this voltage will be generated by the modulator even under extreme DC link voltage unbalance situations. This fact makes the proposed 1D-FFSVM technique very interesting as a way to avoid the undesirable effects of DC link voltage unbalance on the distortion of the output waveforms. In addition, the proposed 1D-FFSVM method has been optimized to include a simple way to control the DC voltage ratio and maintain good performance under transient or steady state DC voltage unbalance. The proposed modulation technique has been introduced using the two-cell topology but it can be easily extended for higher number of cells in the single-phase CHB converter. Experimental results using a 5kVA two-cell single-phase CHB converter are shown in order to validate the proposed modulation techniques.

REFERENCES

[1] M. Marchesoni, M. Mazzucchelli and S. Tenconi, “A non Conventional Power Converter for Plasma Stabilization,” in Power Electronics Specialist Conference 1988 (PESC’88), pp. 122–129, 11-14 April 1988.

[2] J. Rodriguez, Jih-Sheng Lai and Fang Zheng Peng, “Multilevel inverters: a survey of topologies, controls, and applications”, *IEEE Transactions on Industrial Electronics,* Volume 49, Issue 4, pp. 724 – 738, Aug. 2002.

[3] Y. Cheng, C. Qian, M.L. Crow, S. Pekarek and S. Atcitty, "A Comparison of Diode-Clamped and Cascaded Multilevel Converters for a STATCOM With Energy Storage," *IEEE Transactions on Industrial Electronics*, vol. 53, no. 5, pp. 1512-1521, Oct 2006.

[4] M.E. Ortuzar, R.E. Carmi, J.W. Dixon and L. Moran, "Voltage-source active power filter based on multilevel converter and ultracapacitor DC link," *IEEE Transactions on Industrial Electronics*, vol. 53, no. 2, pp. 477- 485, Apr 2006.

[5] M. D. Manjrekar, P. K. Steimer and T. A. Lipo, “Hybrid multilevel power conversion system: a competitive solution for high-power applications”, *IEEE Transactions on Industry Applications*, Volume 36, Issue 3, pp. :834 – 841, May-June 2000.

[6] F. Blaabjerg, J. Pedersen, and P. Thoegersen, “Improved modulation techniques for pwm-vsi drives”, *IEEE Transactions on Industrial Electronics*, vol. 44, no. 1, pp. 87–95, February 1997.

[7] G. Carrara, S. Gardella, M. Marchesoni, R. Salutari, and G. Sciutto, “A new multilevel pwm method: A theoretical analysis,” *IEEE Transactions on Power Electronics*, vol. 7, no. 3, pp. 497–505, July 1992.

[8] B. P. McGrath and D. G. Holmes, “Multicarrier PWM strategies for multilevel inverters”, *IEEE Transactions on Industrial Electronics*, vol. 49, no. 4, pp. 858–867, August 2002.

[9] P. Hammond, “A new approach to enhance power quality for medium voltage drives,” *IEEE Transactions on Industry Applications*, vol. 33, no. 1, pp. 202–208, 1997.

[10] A. K. Gupta and A. M. Khambadkone, “A Space Vector PWM Scheme for Multilevel Inverters Based on Two-Level Space Vector PWM”, *IEEE Transactions on Industrial Electronics,* Volume 53, Issue 5, pp. 1631 – 1639, Oct. 2006.

[11] M. M. Prats, J. M. Carrasco and L. G. Franquelo, “Effective algorithm for multilevel converters with very low computational cost”,*IEEE Electronics Letters*, Volume 38, Issue 22, 24 Oct 2002, pp. 1398 - 1400

[12] N. Celanovic and D. Boroyevich, “A fast space-vector modulation algorithm for multilevel three-phase converters”, *IEEE Transactions on Industry Applications*, Volume 37, Issue 2, pp.:637-641, March-April 2001.

[13] Cassiano Rech, Jos Renes Pinheiro, "Hybrid Multilevel Converters: Unified Analysis and Design Considerations," Trans. on Industrial Electronics, vol. 54, no. 2, pp. 1092-1104, April 2007.

[14] O. Bouhali, E. M. Berkouk, B. Francois and C. Saudemont, "Direct Generalized Modulation of Electrical Conversions Including Self Stabilization of the DC-Link for a Single Phase Multilevel Inverter Based AC Grid Interface", Power Electronics Specialists Conference, 2004 (PESC'04), pp. 1385-1391, 2004.

[15] J. Pou, R. Pindado, D. Boroyevich, P. Rodriguez, and J. Vicente, "Voltage-balancing strategies for diode-clamped multilevel converters", IEEE 2004 Power Electronics Specialist Conference (PESC'04), Volume 5, pp. 3988 – 3993, 20-25 June 2004.
[16] J. I. Leon, G. Guidi, L. G. Franquelo, T. Undeland and S. Vazquez, "Simple Control Algorithm to Balance the DC-Link Voltage in Multilevel Four-Leg Four-Wire Diode Clamped Converters", Proceedings of 12th International Power Electronics and Motion Control Conference (EPE-PEMC'06), pp. 228 – 233, Aug. 2006.
[17] J. I. Leon, R. Portillo, L. G. Franquelo, S. Vazquez, J. M. Carrasco and E. Domínguez, "New space vector modulation technique for single-phase multilevel converters", Proceedings of IEEE International Symposium on Industrial Electronics 2007 (ISIE'07), pp. 617-622, 4-7 June 2007.
[18] N. Celanovic, I. Celanovic and D. Boroyevich, D.; "The feedforward method of controlling three-level diode clamped converters with small DC-link capacitors", in Power Electronics Specialists Conference, 2001 (PESC 2001) IEEE 32nd Annual, Volume 3, pp. 1357 – 1362, 17-21 June 2001.
[19] J. Pou, D. Boroyevich and R. Pindado, "New feedforward space-vector PWM method to obtain balanced AC output voltages in a three-level neutral-point-clamped converter", *IEEE Transactions on Industrial Electronics*, Volume 49, Issue 5, pp.1026-1034, Oct. 2002.
[20] S. Kouro, P. Lezana, M. Angulo and J. Rodriguez, "Multicarrier PWM With DC-Link Ripple Feedforward Compensation for Multilevel Inverters", *IEEE Transactions on Power Electronics*, Volume 23, Issue 1, pp. 52-59, Jan. 2008.
[21] J. Carter, C. J. Goodman, H. Zelaya and S. C. Tran, "Capacitor voltage control in single-phase three-level PWM converters", Fifth European Conference on Power Electronics and Applications 1993, Volume 7, pp. 149 – 154, 13-16 Sep 1993.
[22] A. Chen and X. He, "Research on Hybrid-Clamped Multilevel-Inverter Topologies", *IEEE Transactions on Industrial Electronics,* Volume 53, Issue 6, pp. 1898 – 1907, Dec. 2006.
[23] A. Bendre, G. Venkataramanan, D. Rosene and V. Srinivasan, "Modeling and design of a neutral-point voltage regulator for a three-level diode-clamped inverter using multiple-carrier modulation", *IEEE Transactions on Industrial Electronics,* Volume 53, Issue 3, pp. 718 – 726, June 2006.
[24] L. M. Tolbert, Fang Zheng Peng and T. G. Habetler, "Multilevel PWM methods at low modulation indices", *IEEE Transactions on Power Electronics,* Volume 15, Issue 4, pp. 719 – 725, July 2000.
[25] G. Sinha and T. A. Lipo, "A four-level inverter based drive with a passive front end", *IEEE Transactions on Power Electronics,* Volume 15, Issue 2, pp. 285 – 294, March 2000.
[26] R. Burgos, R. Lai, Y. Pei, F. Wang, D. Boroyevich and J. Pou, "Space Vector Modulation for Vienna-Type Rectifiers Based on the Equivalence between Two- and Three-Level Converters: A Carrier-Based Implementation", in IEEE Power Electronics Specialist Conference 2007 (PESC'07), pp. 2861 – 2867, 17-21 June 2007

Jose I. Leon (S'04, M'07) was born in Cádiz, Spain, in 1976. He received the B.S. and M.S. and PhD degrees in telecommunications engineering from the University of Seville (US), Seville, Spain, in 1999, 2001 and 2006 respectively.
In 2002, he joined the Power Electronics Group, US, working in R+D projects. Currently, he is an Associate Professor with the Department of Electronic Engineering, US. His research interests include electronic power systems, modeling, modulation and control of power-electronics converters and industrial drives, and power quality in renewable generation plants.

Sergio Vazquez (S'04) was born in Seville, Spain, in 1974. He received the B.S. and M.S. degrees in industrial engineering from the University of Seville (US), Seville, Spain, in 2003 and 2006, respectively.
In 2002, he was with the Power Electronics Group, US, working in research and development projects. He is currently an Assistant Professor with the Department of Electronic Engineering, Escuela Superior de Ingenieros, US. His research interests include electronic power systems, modeling, modulation and control of power electronic converters and industrial drives, and power quality in renewable generation plants.

Alan J. Watson (S'03) received the Masters degree in Electrical and Electronic Engineering from the University of Nottingham, UK in 2004.
He is presently pursuing a PhD in Electrical and Electronic Engineering at the University of Nottingham, UK. His research interests include Multilevel Converters, advanced modulation schemes and power converter control.

Leopoldo G. Franquelo (M'84–SM'96–F'05) was born in Málaga, Spain. He received the M.Sc. and Ph.D. degrees in electrical engineering from the University of Seville, Seville, Spain, in 1977 and 1980, respectively. In 1978, he joined the University of Seville and is Professor since 1986. From 1998 to 2005, he has been the Director of the Department of Electronic Engineering.
He was the Vice-President of the Industrial Electronics Society (IES) Spanish Chapter (2002–2003), member at Large of the IES AdCom (2002–2003). He has been the Vice-President for Conferences of the IES since 2004, in which he has also been a Distinguished Lecturer since 2006. He has been an Associated Editor for the IEEE Transactions on Industrial Electronics since 2007.
His current research interest lies on modulation techniques for multilevel inverters and its application to power electronic systems for renewable energy systems. He leads a large research and teaching team in Spain. In last five years, he is author of 40 publications in international journals and 165 in international conferences. He is holder of ten patents and advisor for ten Ph.D. dissertations and 96 R&D projects.

Patrick W. Wheeler (M'00) received his BEng [hons] in 1990 from the University of Bristol, UK. He received his PhD degree in Electrical Engineering for his work on Matrix Converters from the University of Bristol, UK, in 1994. In 1993 he moved to the University of Nottingham and worked as a research assistant in the Department of Electrical and Electronic Engineering. In 1996 he became a Lecturer in the Power Electronics, Machines and Control Group at the University of Nottingham, UK. Since January 2008 he has been a Full Professor in the same research group.
His research interests are are in power converter topologies and their applications. He has published over 200 papers in leading international conferences and journals.

Juan M. Carrasco (M'97) was born in San Roque, Spain. He received the M.Eng. and Dr.Eng. degrees in industrial engineering from the University of Seville, Seville, Spain, in 1989 and 1992, respectively.
From 1990 to 1995, he was an Assistant Professor with the Department of Electronic Engineering, Escuela Superior de Ingenieros, Sevilla University, where he is currently an Associate Professor. He has been working for several years in the power electronic field where he was involved in the industrial application of the design and development of power converters applied to renewable energy technologies. His current research interests are in distributed power generation and the integration of renewable energy sources.